Interaction of atoms with a magneto-optical potential

C. S. Adams, T. Pfau, Ch. Kurtsiefer, and J. Mlynek
Fakultät für Physik, Universität Konstanz, D-7750 Konstanz, Germany
(Received 22 February 1993)

A theoretical study of the coherent interaction of multilevel atoms with a magneto-optical potential is presented. The potential is formed by counterpropagating linearly polarized laser beams whose polarization vectors intersect at an angle φ and a static magnetic field applied parallel to the laser propagation direction. For a particular ratio of the light and magnetic field amplitudes, the light shift at positions of purely circularly polarized light is equal to the Zeeman splitting. In this case, for a three-level atom, one of the eigenvalues has a triangular spatial form. The diffraction of atoms from this triangular phase grating is an efficient beam splitter. The splitting is symmetric for $\varphi=90°$ and asymmetric for $\varphi<90°$. In addition we show that at well-defined positions in the light field, the atom undergoes nonadiabatic transitions and thus by using state-selective detection, one could observe an interference pattern produced by an array of double slits.

PACS number(s): 32.90.+a, 32.80.−t, 42.50.−p

I. INTRODUCTION

The diffraction of two-level atoms from a standing-wave light field is interesting both in the context of our general understanding of light-matter interactions and because of possible applications as coherent beam splitters, which are a key component in the realization of atom interferometers. The first convincing demonstration of the transfer of individual photon momenta between light and atoms was reported by Moskowitz *et al.* in 1983 [1]. Improved results were reported in 1986 [2]. The coherent diffraction process (i.e., no spontaneous emission) can be described either in terms of discrete momentum transfer caused by the scattering of photons, or by refraction of a matter wave from an optical phase grating (or optical potential) arising from the spatial modulation of the light shift. If the transverse motion of the atom is small compared to the optical wavelength, then the wave function accumulates a position-dependent phase shift proportional to the energy of the populated eigenstate. The final momentum distribution is given by the Fourier transform of the phase-shifted wave function. For a standing wave, the eigenvalues are sinusoidal functions of position, i.e., the atom is diffracted by a sinusoidal phase grating, and the final momentum distribution is given by a Bessel-function distribution [3]. For a small phase modulation, e.g., one absorption-stimulated emission cycle, standing-wave diffraction produces efficient scattering into states with $\pm 2\hbar k$. However, for a large phase modulation (many absorption-stimulated emission cycles) a large number of diffraction orders are populated and there is broad spreading rather than a clear splitting of the beam. For this reason, standing-wave diffraction is far from being the ideal beam splitter with just two outputs and a large splitting in momentum space.

In this paper we show that by introducing a further degree of freedom in the light-atom interaction (namely, polarization-selective absorption and emission), it is possible to gain more control of the momentum-transfer process, and for example create an effective scheme for an atomic beam splitter [4]. Two extensions of the normal standing-wave interaction are proposed. First, we allow the atom to distinguish between the counterpropagating laser beams which form the standing wave. This can be achieved using beams with different polarizations and a multilevel atom where the transitions are polarization selective. Second, we introduce a magnetic field in order to switch the atomic coupling from one beam to the other.

To illustrate the momentum-transfer process in this magneto-optical interaction, consider a $J=0$ to $J'=1$ transition. The quantization axis is chosen parallel to the magnetic field. The level scheme is shown in Fig. 1(a). The excitation of the atom by linearly polarized light induces an equal superposition of the $m_{J'}=\pm 1$ levels known as an alignment [depicted schematically by an ellipsoid in Fig. 1(b)]. The direction of the alignment is parallel to the polarization direction. The alignment states does not couple to light polarized perpendicular to the alignment direction. A magnetic field induces a mixing of the excited-state sublevel coherences leading to a precession of the alignment.

Consider an interaction formed by counterpropagating, linearly polarized beams, whose polarization vectors intersect at an angle φ [as shown in Fig. 1(b)]. The precession of the alignment changes probability of absorbing or emitting photons from one beam or the other. If the frequency of the absorption and emission processes is matched to the precession frequency, the atom repeats cycles of absorption from one beam and emission into the other, or vice versa. In this case, the direction of momentum transfer (determined by the first absorption process) is preserved. For orthogonally polarized laser beams, a symmetric splitting of the beam is expected from the symmetry of the laser fields.

The physical mechanism of this effect is analogous to the magneto-optical force proposed and demonstrated by

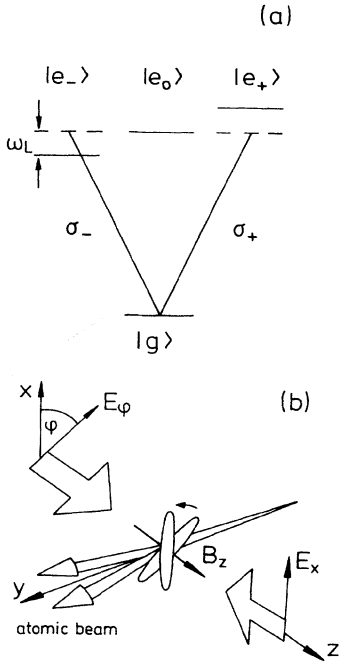

FIG. 1. (a) Level scheme for a $J=0$ to $J'=1$ transition with the quantization axis chosen parallel to the magnetic field. (b) The configuration of the laser fields E_x and E_φ, and the magnetic field B_z, relative to the atomic beam direction (y). The momentum-transfer process is controlled by the Larmor precession of the excited-state alignment (shown schematically as an ellipsoid) and the polarization-dependent selection rules for transitions to the excited state.

Grimm *et al.* [5]. However, the unidirectional magneto-optical force occurs in the regime where the interaction time is much longer than the spontaneous-decay time. In this case the transverse motion of the atom through the potential becomes significant, and the atom experiences an averaged dipole force. The combined effect of spontaneous emission and linearly polarized beams with polarization vectors at an angle $\varphi=45°$ breaks the transverse symmetry between emission and absorption cycles, and there is a net unidirectional force on the atom. In contrast, in this paper we consider the regime where the interaction time is short compared to the spontaneous lifetime (i.e., coherent diffraction), and the change in the transverse motion of the atom induced by the interaction is negligible (i.e., the Raman-Nath approximation). In this regime, the magneto-optical interaction produces a beam splitting.

We present quantum-mechanical calculations of the coherent diffraction of multilevel atoms from a magneto-optical grating. For a particular ratio of the laser intensity and magnetic field strength, we show that one of the eigenstates of the interaction experiences an approximately triangular potential resulting in a large, clearly two-peaked splitting in the momentum state of the atom. For this eigenstate the optical potential changes from a symmetric triangular function for $\varphi=90°$, to an asymmetric or sawtooth function for $\varphi=45°$. The gradient of the potential, which determines the splitting angle, is proportional to the laser and magnetic field amplitudes. For a $J=0$ to $J'=1$ transition, under experimentally realistic conditions, the ground state evolves adiabatically into the split eigenstate and then back to the ground state [6]. For a $J=1$ to $J'=0$ transition, the atom must be prepared in the excited state to observe an efficient splitting. As this is more difficult to achieve experimentally, the $J=0$ to $J'=1$ transition will be the main focus of this paper. The extension of the magneto-optical interaction to a $J=1$ to $J'=2$ transition is considered. This example demonstrates the influence of different light couplings between substates.

The influence of nonadiabatic processes in the magneto-optical interaction was considered by solving the Schrödinger equation for the internal motion of the atom as a function of position in the light field. For a Gaussian laser profile and an interaction involving many absorption and emission cycles, the probability for an atom to make a nonadiabatic transition is less than a few percent, therefore adiabatic evolution is a good approximation. Nonadiabatic transitions mainly occur near positions of σ_+ or σ_- polarization, when the light shift is equal to the Zeeman splitting. For an incident plane matter wave, this leads to a spatially dependent excitation probability with the form of an array of double slits. Diffraction effects resulting from nonadiabatic passage will be discussed.

The paper is organized as follows: In Sec. II the theory of the magneto-optical interaction is discussed in terms of the eigenvalues of the interaction Hamiltonian. In Sec. III the momentum distribution produced by diffraction from a magneto-optical potential is calculated. The calculations are simplified by assuming adiabatic evolution. In this case the interaction can be treated as a phase grating. The validity of the adiabatic approximation and the effect of nonadiabatic transitions are discussed in Sec. IV. The paper concludes with a brief summary (Sec. V).

II. MAGNETO-OPTICAL EIGENVALUES AND EIGENSTATES

The precessing alignment model of the magneto-optical interaction described in the introduction is an oversimplification as the alignment does not evolve freely and the absorption and emission processes do not occur instantaneously, i.e., the time evolution of the magnetic and light interaction are coupled and cannot be treated separately. A more accurate physical insight into the role of the magnetic and laser fields is provided by considering the eigenstates of the interaction in position representation. Again we stress that spontaneous emission is neglected.

We consider a $J=0\rightarrow J'=1$ transition and choose the quantization axis parallel to the magnetic field direction [i.e., along z in Fig. 1(b)]. In this basis the $|e_0\rangle$ sublevel does not interact with the laser or the magnetic field, and the level scheme reduces to a three-level system [Fig. 1(a)].

The wave function of the atom in the position representation may be written as

$$|\Psi\rangle=\sum_i \int \psi_i(\mathbf{r},t)|i\rangle|\mathbf{r}\rangle d\mathbf{r} , \tag{1}$$

where $i=\{g_0,e_-,e_+\}$ is the internal state and $\mathbf{r}$ is the center of mass position.

For this problem the total Hamiltonian is the sum of the atomic Hamiltonian H_{atom}, the magnetic field interaction H_B, and the atom-laser coupling H_{a-l}. The atomic Hamiltonian is a sum of the kinetic energy of the atom, and the internal energy given by the population of the excited levels:

$$H_{\text{atom}}=\frac{p^2}{2m}+\hbar\omega_0(|e_+\rangle\langle e_+|+|e_-\rangle\langle e_-|) , \tag{2}$$

where ω_0 is the unperturbed atomic transition frequency. The calculations are greatly simplified, if the kinetic energy term in H_{atom} can be neglected, i.e., if the change in the kinetic energy of the atom induced by the interaction is negligible. This is known as the Raman-Nath approximation. In the position representation the Raman-Nath regime can be interpreted as the limit where the change in the trajectory of the atom induced by the interaction is small compared to the wavelength of the light. The Raman-Nath assumption places an upper limit on the maximum momentum splitting we are able to predict using our model.

The magnetic interaction is given by

$$H_B=-\boldsymbol{\mu}\cdot\mathbf{B} , \tag{3}$$

where $\boldsymbol{\mu}=-g_J\mu_B\mathbf{J}$ is the magnetic moment. The magnetic field is parallel to the quantization axis, therefore H_B has only diagonal elements corresponding to the Zeeman shift. The atom-laser interaction in the electric dipole approximation is given by

$$H_{a-l}=-\mathbf{d}\cdot\text{Re}\{\mathbf{E}(\mathbf{r})e^{-i\omega_{\text{laser}}t}\} , \tag{4}$$

where $\mathbf{d}$ is the electric dipole operator and the laser amplitude $\mathbf{E}(\mathbf{r})$ is

$$\mathbf{E}(\mathbf{r})=E_0(x,y)[(\hat{\boldsymbol{\epsilon}}_x\cos\varphi+\hat{\boldsymbol{\epsilon}}_y\sin\varphi)e^{ikz}+\hat{\boldsymbol{\epsilon}}_x e^{-ikz}] , \tag{5}$$

where φ is the angle between the polarization vectors of the two beams. The atomic beam propagates in the y direction [see Fig. 1(b)]. The spatial dependence of $E_0(x,y)$ along y, in the moving frame of the atom, can be written as an explicit time dependence $t=y/v$ where v is the velocity of the atom. For simplicity we assume that the field is uniform along x. To simplify, the light couplings in the chosen basis of magnetic substates, the electric field is rewritten in terms of the σ_+ and σ_- polarization components, i.e.,

$$\mathbf{E}(vt)=\sqrt{2}E_0(vt)[\hat{\boldsymbol{\epsilon}}_+e^{-i\varphi/2}\cos(kz-\varphi/2) +\hat{\boldsymbol{\epsilon}}_-e^{i\varphi/2}\cos(kz+\varphi/2)] . \tag{6}$$

It follows from (6) that the polarization gradient is equivalent to the superposition of a σ_+ and a σ_- standing-wave field with a spatial displacement of $\varphi\lambda/2\pi$ [5]. By making the rotating-wave approximation and for a laser detuning $\Delta=\omega_{\text{laser}}-\omega_0$ where ω_0 is the unperturbed transition frequency, the Hamiltonian in the interaction representation reduces to the sum of the magnetic interaction and the atom-light coupling. From Eqs. (1)–(6) it follows that the interaction Hamiltonian for the state vector $\{g_0,e_-,e_+\}$ is

$$H_{\text{int}}=\hbar\begin{bmatrix}\Delta & G_- & G_+\\ G_-^* & -\omega_L & 0\\ G_+^* & 0 & \omega_L\end{bmatrix} , \tag{7}$$

where $G_\pm=(\omega_R(t)/\sqrt{2})e^{\pm i\varphi/2}\cos(kz\pm\varphi/2)$, the Rabi frequency $\omega_R(t)$ is defined as [7]

$$\omega_R(t)=-\frac{\langle e_\pm|\mathbf{d}\cdot\hat{\boldsymbol{\epsilon}}_\pm|g_0\rangle}{\hbar}E_0(vt) \tag{8}$$

and $\hbar\omega_L=g_J\mu_B B$ is the Zeeman splitting.

The eigenvalues of the interaction Hamiltonian are given by the roots of the characteristic equation as

$$\lambda_j=\frac{2}{3}\hbar(\Delta^2+3B)^{1/2}\cos\left\{\frac{1}{3}\cos^{-1}\left[\frac{27C+2\Delta^3-9\Delta(B-3\omega_L^2)}{2(\Delta^2+3B)^{3/2}}\right]+\frac{2\pi j}{3}\right\}-\frac{\hbar\Delta}{3} , \tag{9}$$

where $B=\omega_L^2+(\omega_R^2/2)[1+\cos\varphi\cos(2kz)]$, $C=(\omega_L\omega_R^2/2)\sin(\varphi)\sin(2kz)$ and $j=1$, 2, or 3.

The eigenstates can be written as

$$|j\rangle=\alpha_{j0}|g_0\rangle+\alpha_{j-}|e_-\rangle+\alpha_{j+}|e_+\rangle , \tag{10}$$

where the non-normalized eigenvector components are given by

$$\alpha_{j0}=(\hbar\omega_L+\lambda_j)(\hbar\omega_L-\lambda_j) , \tag{11}$$

$$\alpha_{j-}=\hbar G_-^*(\hbar\omega_L-\lambda_j) , \tag{12}$$

$$\alpha_{j+}=-\hbar G_+^*(\hbar\omega_L+\lambda_j) . \tag{13}$$

Similar expressions for a three-level system driven by two light fields with arbitrary detunings have been derived previously [8].

Below the spatial structure of the eigenvalues will be discussed with reference to specific examples. In Fig. 2 the eigenvalues λ_j for $\varphi=90°$ are plotted as a function of position in the polarization gradient. First we consider the eigenvalues for zero laser detuning, $\Delta=0$ [shown in Figs. 2(a) and 2(b)]. In a weak laser field [Fig. 2(a)], the eigenstates $|1\rangle$, $|2\rangle$, and $|3\rangle$ correspond approximately to the magnetic eigenstates, i.e., to the initial states $|e_-\rangle$, $|g_0\rangle$, and $|e_+\rangle$, respectively. The separation of the eigenvalues is equal to the Zeeman splitting of the excited state and their spatial modulation is due to the light shift, which is proportional to the intensity of the σ_+ or σ_-

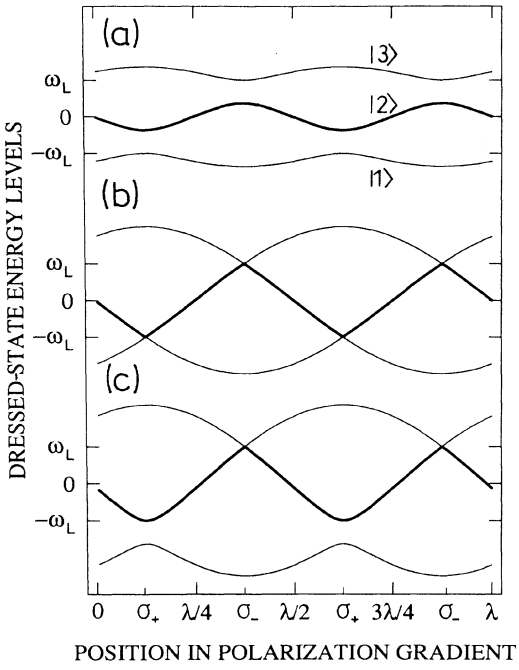

FIG. 2. Spatial dependence of the eigenvalues for a $J=0$ to $J'=1$ transition and $\varphi=90°$: (a) $\omega_R=\omega_L$, $\Delta=0$, (b) $\omega_R=2\omega_L$, $\Delta=0$, and (c) $\omega_R=\sqrt{6}\omega_L$, $\Delta=\omega_L/2$.

field component. In the strong laser field (or weak magnetic field) case, the eigenstates correspond to mixtures of the magnetic sublevels which are separated by the light shift and modulated due to the magnetic perturbation. In the limit $\omega_L\to 0$ (i.e., no magnetic field) the light shift of the eigenstates becomes independent of position, because the σ_+ and σ_- couplings are equal.

For $\omega_R=2\omega_L$ the light shift on the $\sigma_\pm$ transition, at the position of pure $\sigma_\pm$ polarized light (indicated below in Fig. 2), is exactly sufficient to bring the $\sigma_\mp$ transition to resonance, and the level anticrossing shows a degeneracy [Fig. 2(b)]. In this case the first-order perturbation induced by a small σ_- or σ_+ component does not vanish (in contrast to the nondegenerate case), and therefore due to the linear increase of the $\sigma_\mp$ component on either side of the anticrossing, and levels are perturbed linearly along z. Thus eigenstate $|2\rangle$ has an eigenvalue with approximately triangular spatial dependence [shown by the thicker line in Fig. 2(b)]. An atom in eigenstate $|2\rangle$ experiences an optical potential with triangular spatial dependence which leads to an efficient splitting in the momentum state of the atom (the diffraction pattern will be calculated in Sec. III). The magnitude of the deflecting force is given by the potential gradient. It can be seen from Fig. 2(b) that the magnitude of the gradient is approximately the Zeeman splitting $2\hbar\omega_L$ divided by $\lambda/4$. Thus the deflecting force is approximately $\pm 8\hbar k\omega_L/2\pi$. The other eigenstates display a more sinusoidal spatial dependence and therefore give rise to a diffraction pattern similar to that produced by a normal standing wave.

The interaction is relatively insensitive to the atom-laser detuning: The eigenvalues are not significantly perturbed until the detuning becomes comparable to the characteristic frequencies ω_R or ω_L. In Fig. 2(c) the magneto-optical eigenvalues for $\Delta=\omega_L/2$ are plotted. The effect of the detuning is to shift the energy of the central eigenstate. The consequence of the asymmetric energy level spacings is that the degeneracies at the $\sigma_\pm$ polarization positions occur at different Rabi frequencies. For a positive detuning, fir the σ_+ light shift brings eigenvalues $|2\rangle$ and $|3\rangle$ to degeneracy, then at a higher laser power the σ_- transition brings eigenstates $|1\rangle$ and $|2\rangle$ to degeneracy. The relationship between the Rabi frequency, the Larmor frequency, and the detuning, to achieve degeneracy at the $\sigma_\pm$ positions, is

$$\tfrac{1}{2}[2\omega_R^2+(\omega_L\pm\Delta)^2]^{1/2}-\tfrac{1}{2}(\omega_L\pm\Delta)=\omega_L\mp\Delta\ . \tag{14}$$

Note that $\sqrt{2}\omega_R$ is the Rabi frequency for a $|\Delta m_J|=1$ transition at the $\sigma_\pm$ polarization positions. In Fig. 2(c), $\Delta=\omega_L/2$ and the degeneracy at σ_- polarization positions is $\omega_R=\sqrt{6}\omega_L$.

The effect of changing the angle φ is to slide the spatial dependence of the σ_+ light shift relative to the σ_- light shift. This is illustrated in Fig. 3 where the eigenvalues for $\varphi=45°$ and $\varphi=-22.5°$ are plotted as a function of position in the polarization gradient. In Fig. 3 the ratio of ω_R and ω_L was chosen according to the anticrossing degeneracy condition for arbitrary angle φ:

$$\omega_R=\frac{2}{\sin\varphi}\omega_L\ . \tag{15}$$

It follows from (15) that higher laser intensities are required to produce degeneracy for smaller angles. For $\varphi<90°$ the eigenvalue of the adiabatically populated eigenstate has a sawtooth structure. Thus an asymmetric

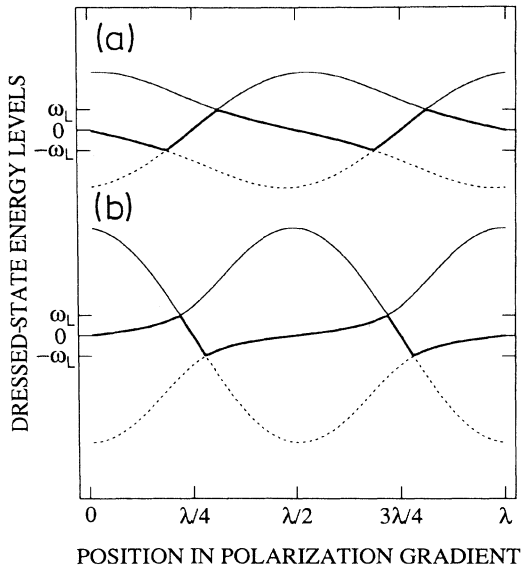

FIG. 3. Spatial dependence of the eigenvalues for a $J=0$ to $J'=1$ transition and $\Delta=0$: (a) $\varphi=45°$ and (b) $\varphi=-22.5°$ with $\omega_R=2\omega_L/\sin\varphi$.

beam-splitting effect is expected. The sign of the asymmetry depends on the sign of φ and the sign of the magnetic field. The same symmetry behavior has been observed in connection with the unidirectional magneto-optical force [4].

In order to extend the discussion to more complex atoms, we have calculated the magneto-optical eigenvalues for atoms with a $J=1$ to $J'=2$ transition resonant ($\Delta=0$) with the light field. For two linearly polarized beams and an axial magnetic field, the level structure can be separated into a W system and a V system which are uncoupled. The V system behaves as discussed above. The level scheme for the W system is depicted in Fig. 4(a). The wave function of the W system can be written as the state vector in the basis $\{|e_{-2}\rangle,|g_{-1}\rangle,|e_0\rangle,|g_{+1}\rangle,|e_{+2}\rangle\}$. The interaction Hamiltonian for zero laser detuning is

$$H_{\rm int}=\hbar\begin{bmatrix} -\frac{3}{2}\omega_L & G_-^* & 0 & 0 & 0 \\ G_- & -\omega_L & \frac{1}{\sqrt{6}}G_+ & 0 & 0 \\ 0 & \frac{1}{\sqrt{6}}G_+^* & 0 & \frac{1}{\sqrt{6}}G_-^* & 0 \\ 0 & 0 & \frac{1}{\sqrt{6}}G_- & \omega_L & G_+ \\ 0 & 0 & 0 & G_+^* & \frac{3}{2}\omega_L \end{bmatrix}, \tag{16}$$

where $G_\pm$ are the light-atom couplings for a Clebsch-Gordon coefficient of unity, as defined in Eq. (7), and ω_L is the Zeeman splitting in the ground state. Note that the ground and excited states have different g_J factors; in this example we have assumed a $^3S_1$ to $^3P_2$ transition, for example as found in metastable helium.

The eigenvalues were calculated numerically. The eigenvalues for $\varphi=90°$ as a function of position in the polarization gradient are shown in Fig. 5. The five-level system is significantly more complicated that the three-level case. For example, there are now three degeneracy conditions. The relationship between ω_L and ω_R corresponding to each degeneracy is easily derived by equating the effective level shifts and the appropriate Zeeman splitting. Expressions similar to the nonresonant three-level case [Eq. (14)] are obtained. The first degeneracy occurs at positions of $\sigma_\pm$ polarized light when the combined light shifts of the $|g_{\mp1}\rangle\rightarrow|e_0\rangle$ and $|g_{\pm1}\rangle\rightarrow|e_{\pm2}\rangle$ transitions exactly compensate for the Zeeman splitting between $|g_{\pm1}\rangle$ and $|e_0\rangle$ [Fig. 5(a)]. The degeneracy condition is $\omega_R\sim1.499\omega_L$. The second degeneracy occurs at $\omega_R=3\omega_L$ where the $|g_{\pm1}\rangle\rightarrow|e_0\rangle$ light shift is equal to the Zeeman splitting between $|g_{\pm1}\rangle$ and $|e_{\pm2}\rangle$. The third degeneracy occurs at $\omega_R=\sqrt{15}\omega_L$ [Fig. 5(b)] when the light shifts of the $|g_{\pm1}\rangle\rightarrow|e_{\pm2}\rangle$ transition exactly compensates for the Zeeman splitting between $|g_{\pm1}\rangle$ and $|e_{\mp2}\rangle$. This is a three-photon process as shown by the dashed line in Fig. 4(b). The higher-order nature of this process explains the nonlinear divergence of the energy levels on either side of the anticrossing [see Fig. 5(b)]. For $\omega_R\gg\omega_L$ the central eigenstate is associated with a triangular optical potential [Fig. 5(c)]. The triangular

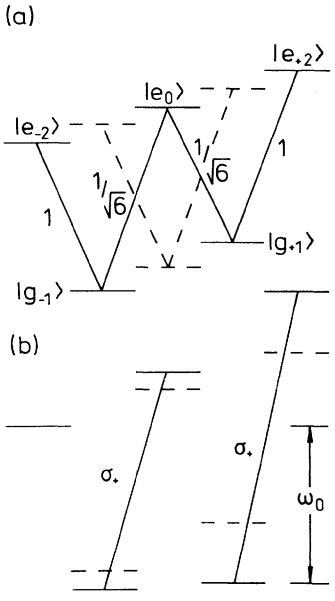

FIG. 4. (a) Level scheme for a $J=1$ to $J'=2$ transition showing the Zeeman shifts of the substates. (b) The influence of a strong σ_+ coupling ($\omega_R=\sqrt{15}\omega_L$) is depicted. The light shifts of the $|g_{+1}\rangle\rightarrow|e_{+2}\rangle$ transition exactly compensates for the Zeeman splitting between $|g_{+1}\rangle$ and $|e_{-2}\rangle$.

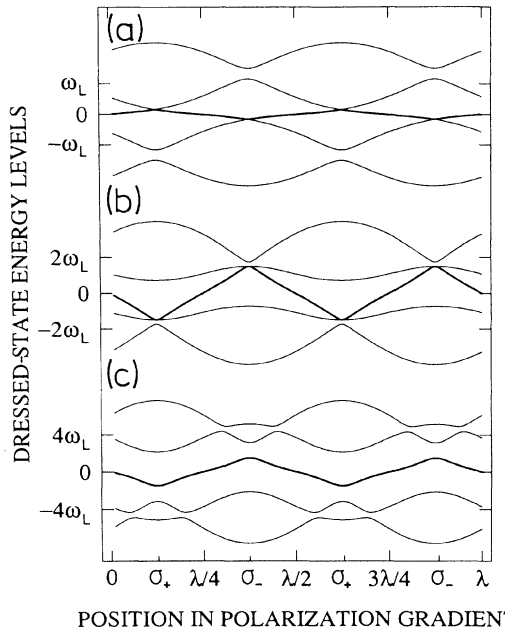

FIG. 5. The spatial dependence of the eigenvalues for the W system in a $J=1$ to $J'=2$ transition with orthogonal polarizations $\varphi=90°$ and (a) $\omega_R\sim1.499\omega_L$, (b) $\omega_R=\sqrt{15}\omega_L$, and (c) $\omega_R=9\omega_L$.

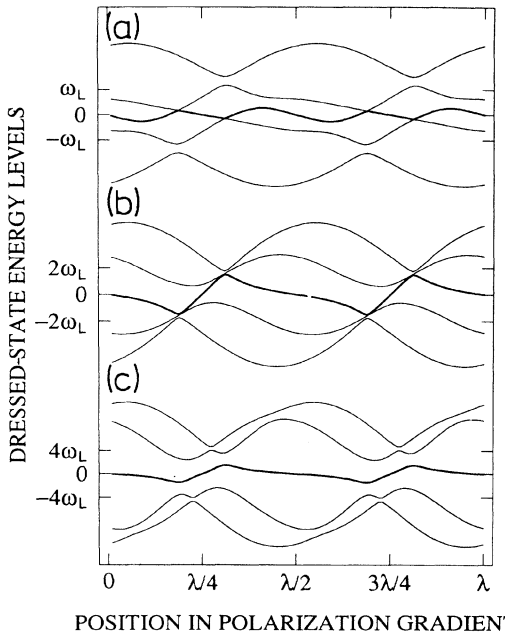

FIG. 6. The spatial dependence of the eigenvalues for the W system in a $J=1$ to $J'=2$ transition with $\varphi=45°$ and (a) $\omega_R \sim 1.499\sqrt{2}\omega_L$, (b) $\omega_R = 4\sqrt{2}\omega_L$, and (c) $\omega_R = 9\sqrt{2}\omega_L$.

form is maintained for a large range of the ratio between the Rabi frequency and the Larmor frequency. This may be convenient in relation to an experimental realization of a magneto-optical beam splitter. However, in contrast to the three-level system, the split state cannot be populated by adiabatic evolution (see Sec. III) due to the repeated occurrence of degeneracy points causing nonadiabatic transitions. Finally we note that the transitions from $|g_{-1}\rangle$ or $|g_{+1}\rangle$ to the excited state have unequal Clebsch-Gordon coefficients, i.e., unequal $\sigma_\pm$ coupling strengths. This asymmetric coupling leads to structure in the optical potential with a periodicity smaller than $\lambda/2$ [Fig. 5(c)] and is also responsible for a nonvanishing potential when the magnetic field is turned off ($\omega_L=0$).

The eigenvalues in the case of $\varphi=45°$ are illustrated in Fig. 6. Again there are three degeneracy conditions. Two examples are shown in Figs. 6(a) and 6(b). For strong light coupling the central eigenvalue shows the same sawtooth structure [Fig. 6(c)] as in the case of a three-level atom. This similarity of the structure of the optical potential in the three- and five-level examples indicates that in the regime where spontaneous emission plays a significant role, we would expect a unidirectional force with similar properties as discussed previously [4].

III. DIFFRACTION OF ATOMS FROM A MAGNETO-OPTICAL POTENTIAL

The diffraction of atoms from a magneto-optical grating in the Raman-Nath regime may be calculated by integrating the Schrödinger equation in position representation using the interaction Hamiltonian given by (7). For simplicity we return to the three-level V system. As the Raman-Nath limit is specific to a particular atomic system, we choose to make the calculations using parameters corresponding to a supersonic beam of metastable helium atoms and a light field resonant with the $2\,^3S_1$ to $2\,^3P_1$ transition. We assume that the atoms are prepared in the $m_J=0$ ground-state level, in which case the problem is identical to the $J=0$ to $J'=1$ transition discussed in Sec. II. In order to remain in the Raman-Nath regime we limit the maximum transverse displacement of the atom to one-tenth of the period of the optical potential.

Before solving the Schrödinger equation, we note that if the switching times of the interaction are slow compared to the characteristic time scale of the magneto-optical process (ω_L or ω_R), then the ground state $|g_0\rangle$ evolves adiabatically into eigenstate $|2\rangle$. In this case the momentum distribution may be calculated by considering the eigenvalue potential as a phase grating. The momentum distribution for an incident plane matter wave is given by the Fourier transform of $\exp[i\int\lambda_2(z,t)dt/\hbar]$ where λ_2 is the nearly triangular shaped eigenvalue. The momentum distribution produced by diffraction from a triangular phase grating for $\int\omega_R(t)dt=20\pi$ is shown in Fig. 7(a). In this example, the magneto-optical interaction behaves as an extremely efficient beam splitter with a momentum splitting of approximately $\pm 40\hbar k$. There is a small amount of scattering into adjacent momentum

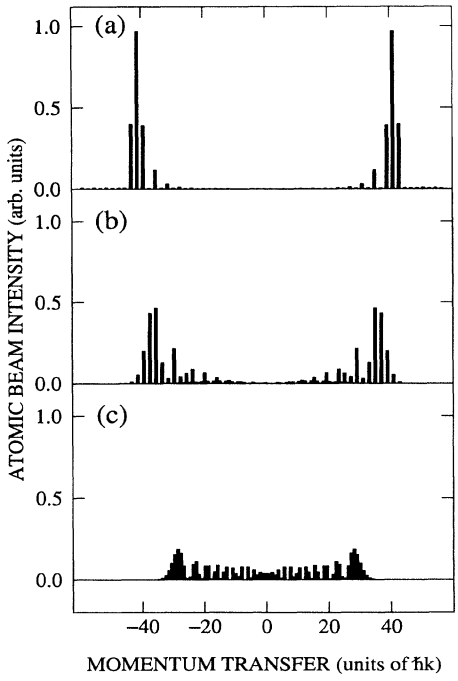

FIG. 7. The final momentum distribution for an atom diffracted by a magneto-optical potential with $\varphi=90°$ and a modulation $\int\omega_R(t)dt=20\pi$ for (a) uniform laser and magnetic fields and perfect adiabatic evolution, (b) a Gaussian laser field calculated by integrating the Schrödinger equation; and (c) for comparison, the momentum distribution produced by diffraction of a two-level atom from a standing-wave light field for the same modulation.

states due to the finite width of the linear regions of the optical potential. The application of the magneto-optical interaction to realize a beam splitter for atom interferometry has been discussed in [4]. The split atomic beam leaves the interaction region in the ground state, i.e., the interaction behaves as a nonpolarizing beam splitter, which is ideal for applications in atom interferometry and an advantage over other beam-splitting effects where the outgoing states are orthogonal.

The example discussed above, where the laser and magnetic fields remain constant throughout the interaction, is difficult to realize experimentally. An experimentally more realistic configuration consists of a Gaussian-profile light field and an approximately uniform magnetic field. The expected momentum distribution for this case, calculated by integrating the Schrödinger equation is shown in Fig. 7(b). The light field and interaction time are again chosen such that $\int \omega_R(t)dt = 20\pi$ and the Rabi frequency at the center of the laser beam is given by $\omega_R = 2.1\omega_L$, such that the degeneracy condition [Eq. (15)] is satisfied twice during the interaction. As the degeneracy condition is not maintained throughout the interaction there is an increase in the population of the lower-order momentum states. If an atom undergoes a nonadiabatic transition it emerges in the excited state. Thus the importance of nonadiabatic processes is indicated by the population of the excited states, i.e., the odd momentum orders in the diffraction pattern. For the parameters used in this example the population of the odd momentum orders and hence the probability of nonadiabatic processes is a few percent [see Fig. 7(b)].

For comparison, the diffraction pattern from a normal standing wave with zero laser detuning, and the corresponding optical potential amplitude is shown in Fig. 7(c). In this case the final momentum distribution is not strongly dependent on the laser profile because the shape of the optical potential does not change significantly with the light intensity. The envelope of the diffraction pattern is the square of a Bessel function. Thus after many Rabi periods there is a broad spread in momentum rather than a clear splitting into high-order momentum states. In contrast, the magneto-optical interaction produces a clearly two-peaked envelope, i.e., it leads to an efficient beam splitting into high-order momentum states.

The calculated momentum distributions to $\varphi = 45°$ and $\varphi = -22.5°$ assuming adiabatic evolution and constant fields are shown in Fig. 8. The diffraction pattern is asymmetric with the majority of the atoms being diffracted in one direction and a smaller amount being diffracted to a larger momentum in the other direction. The asymmetry in the momentum distribution is inverted when φ changes sign. For small φ, a small fraction of the atoms are diffracted to very high momentum states. The net force exerted by the interaction is always zero because the phase grating is periodic, i.e., the center-of-mass momentum is conserved.

IV. NONADIABATIC EFFECTS

The influence of nonadiabatic effects was calculated by integrating the Schrödinger equation for the internal motion as a function position in the polarization gradient. For all calculations discussed in this section, the two laser beams were orthogonally polarized, the magnetic field was uniform, and a Gaussian laser profile was assumed. The total interaction time and the laser intensity were the same as the $\varphi = 90°$ example of Sec. III, i.e., $\int \omega_R(t)dt = 20\pi$. The resonance condition was satisfied at the center of the laser beam, i.e., $\omega_{R\max} = 2\omega_L$.

We assume an incident plane matter wave in the

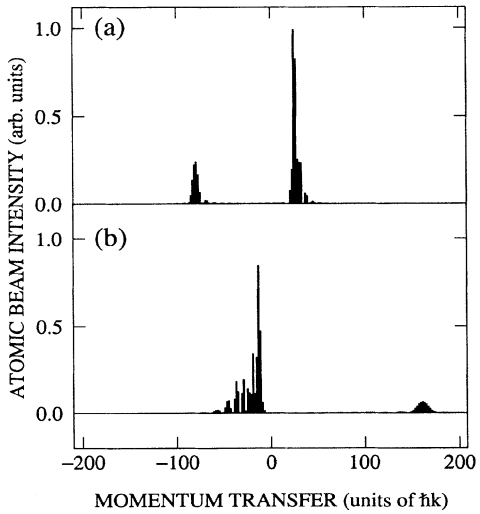

FIG. 8. The final momentum distribution in the adiabatic limit for an atom diffracted by a magneto-optical potential with (a) $\varphi = 45°$ and (b) $\varphi = -22.5°$ for an interaction time $\int \omega_R(t)dt = 20\pi$.

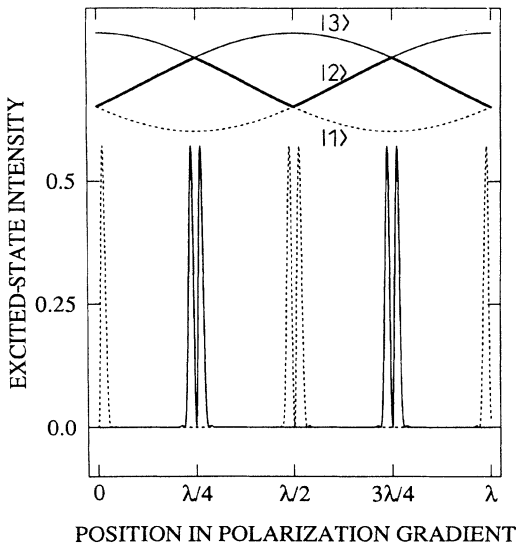

FIG. 9. The excited-state intensity as a function of position in the polarization gradient for an interaction time $\int \omega_R(t)dt = 20\pi$. The eigenvalues are shown inset. The $|e_+\rangle$ and $|e_-\rangle$ state populations and their corresponding eigenvalues are shown as solid and dashed lines, respectively.

ground state and calculate the probability for the atom to leave the interaction in one of the excited states as a function of the position in the polarization gradient. The result is shown in Fig. 9. It can be seen that nonadiabatic transitions are only possible in the vicinity of the level anticrossings. Thus by observing excited atoms, the magneto-optical interaction provides a technique to prepare well-localized atomic wave packets.

Near the σ_- polarization positions, the atomic undergoes a transition from state $|2\rangle$ to $|3\rangle$ (shown as a dashed line in Fig. 9) and consequently emerges from the interaction in $|e_-\rangle$. Similarly near the σ_+ polarization positions, the atom makes a transition from state $|2\rangle$ to $|1\rangle$ and consequently emerges from the interaction in $|e_+\rangle$. At exactly the anticrossing position even though the two eigenstates are degenerate (i.e., the laser is exactly resonant with the transition frequency between the levels) there are no transitions because there is no light component with the correct polarization to drive the transition. The laser field is purely circularly polarized with the opposite polarity to that required to couple the degenerate levels. Thus the spatial probability for nonadiabatic transitions has the form of an array of closely spaced double slits. In this example the width of each "slit" was approximately 0.015λ and the maximum intensity of the excited-state component was ~ 0.55. The total probability for an atom to make a nonadiabatic transition was 6%. This value justifies the validity of the adiabatic approximation used in Sec. III. If the laser intensity and the magnetic field are reduced but the width of the Gaussian beam is kept constant, the rate of absorption and emission decreases and becomes closer to the rate of change of the optical potential. In this case the regions of nonadiabatic behavior become broader. For $\int \omega_R(t)dt = 4\pi$ the probability for nonadiabatic transition increases to 20%.

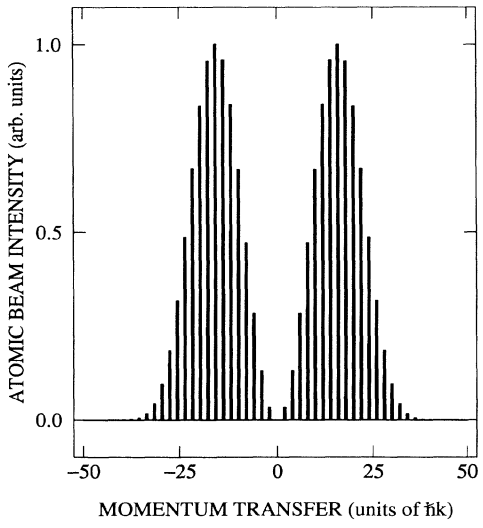

FIG. 10. The momentum distribution for atoms emerging in the excited state. The interference pattern correspond to diffraction from the array of double slits shown in Fig. 9.

By observing only atoms emerging in the excited state, it should be possible to observe the diffraction pattern from the array of double slits shown in Fig. 9. The momentum distribution of the excited-state atoms is plotted in Fig. 10. The envelope of the diffraction pattern consists of the convolution of the single-slit diffraction pattern and the interference pattern due to the double slits. The individual peaks are separated by $2\hbar k$ due to the $\lambda/2$ periodicity of the grating (the grating consists of a $|e_-\rangle$ and a $|e_+\rangle$ component offset by $\lambda/4$, however, the components do not interfere and thus a $\lambda/2$ periodicity is observed). There is not a central maximum in the interference pattern because the excited-state component in the initial eigenstate $|2\rangle$, given by Eqs. (12) and (13) changes sign on either side of the anticrossing.

This example illustrates the possibility offered by the magneto-optical interaction to control the spatial probability of nonadiabatic transitions. In a resonant light-atom interaction the eigenenergy levels are normally degenerate and repel inside the interaction region. Therefore nonadiabatic effects occur as the light field turns on and again when it turns off. In contrast, for the magneto-optical interaction the eigenenergy levels are nondegenerate due to the magnetic field and are brought to degeneracy by the light interaction, i.e., the levels effectively attract within the interaction region.

V. CONCLUSION

We have presented a theoretical study of the coherent scattering of atoms from a magneto-optical potential. For an atom with a $J=0$ to $J'=1$ transition resonant with a light field and for a particular ratio of the laser intensity and the magnetic field strength, there is a degeneracy in the eigenvalues leading to a triangular optical potential. Diffraction from this potential leads to a large splitting in the momentum state of the atom. In contrast to diffraction from a normal standing wave, the magneto-optical interaction produces an efficient splitting to high-order momentum states. The splitting is symmetric when the linearly polarized beams are orthogonal $\varphi = 90°$ and asymmetric for $\varphi < 90°$. For experimental parameters applicable to helium, we predict a splitting of $\pm 40\hbar k$.

The generalization to other transitions was discussed. For a $J=1$ to $J'=2$ transition the level scheme can be separated into a five-level W and three-level V systems. The first-level energy eigenvalues have a similar structure to the three-level case. However, the adiabatic evolution of the atom is complicated due to the occurrence of three degeneracy points as the light coupling is increased. Thus in contrast to the three-level system an efficient beam-splitting effect is not observed.

Finally the influence of nonadiabatic effects was considered. It was shown that for a Gaussian laser beam and an interaction involving many absorption-emission cycles, the number of atoms making nonadiabatic transitions is less than a few percent. Nonadiabatic transitions are restricted to regions of predominantly circularly polarized light and thus by detecting only one internal state,

it is possible to prepare well-localized atomic wave packets. Illumination by a plane matter wave produces a momentum distribution corresponding to diffraction by an array of double slits. This example illustrates the interesting possibility offered by the magneto-optical interaction, to control both the spatial and temporal probability of nonadiabatic processes.

ACKNOWLEDGMENTS

We would like to thank C. Cohen-Tannoudji, T. Sleator, and R. Grimm for fruitful discussions. CSA gratefully acknowledges the support of the Royal Society's European Science Exchange Program. This work is supported by the Deutsche Forschungsgemeinschaft.

[1] P. E. Moskowitz, P. L. Gould, S. R. Atlas, and D. E. Pritchard, Phys. Rev. Lett. **51**, 370 (1983).

[2] P. L. Gould, G. A. Ruff, and D. E. Pritchard, Phys. Rev. Lett. **56**, 827 (1986).

[3] R. J. Cook and A. F. Bernhardt, Phys. Rev. A **18**, 2533 (1978).

[4] T. Pfau, C. S. Adams, and J. Mlynek, Europhys. Lett. **21**, 439 (1993).

[5] R. Grimm, Yu. B. Ovchinnikov, A. I. Sidorov, and V. S. Letokhov, Opt. Commun. **84**, 18 (1991); R. Grimm, V. S. Letokhov, Yu. B. Ovchinnikov, and A. I. Sidorov, Pis'ma Zh. Eksp. Teor. Fiz. **54**, 611 (1991) [JETP Lett. **54**, 615 (1991)]; R. Grimm, V. S. Letokhov, Yu. B. Ovchinnikov, and A. I. Sidorov, J. Phys. (France) II **2**, 93 (1992).

[6] T. Sleator (private communication).

[7] Note that ω_R is defined as the one-beam Rabi frequency.

[8] P. M. Radmore and P. L. Knight, J. Phys. B **15**, 561 (1982).